Histone carbonylation *in vivo* and *in vitro*

Georg T. WONDRAK*, Daniel CERVANTES-LAUREAN†, Elaine L. JACOBSON†‡§ and Myron K. JACOBSON*‡§[1]

*College of Pharmacy, University of Kentucky, Lexington, KY 40506-0286, U.S.A., †Department of Clinical Sciences, University of Kentucky, Lexington, KY 40506-0286, U.S.A., ‡Lucille P. Markey Cancer Center, University of Kentucky, Lexington, KY 40506-0286, U.S.A., and §Advanced Science and Technology Commercialization Center, University of Kentucky, Lexington, KY 40506-0286, U.S.A.

Non-enzymic damage to nuclear proteins has potentially severe consequences for the maintenance of genomic integrity. Introduction of carbonyl groups into histones *in vivo* and *in vitro* was assessed by Western blot immunoassay and reductive incorporation of tritium from radiolabelled $NaBH_4$ (sodium borohydride). Histone H1 extracted from bovine thymus, liver and spleen was found to contain significantly elevated amounts of protein-bound carbonyl groups as compared with core histones. The carbonyl content of nuclear proteins of rat pheochromocytoma cells (PC12 cells) was not greatly increased following oxidative stress induced by H_2O_2, but was significantly increased following alkylating stress induced by *N*-methyl-*N*′-nitro-*N*-nitrosoguanidine or by combined oxidative and alkylating stress. Free ADP-ribose, a reducing sugar generated in the nucleus in proportion to DNA strand breaks, was shown to be a potent histone H1 carbonylating agent in isolated PC12 cell nuclei. Studies of the mechanism of histone H1 modification by ADP-ribose indicate that carbonylation involves formation of a stable acyclic ketoamine. Our results demonstrate preferential histone H1 carbonylation *in vivo*, with potentially important consequences for chromatin structure and function.

Key words: ADP-ribose, glycation, ketoamine, alkylating stress, PC12.

INTRODUCTION

Non-enzymic damage to proteins contributes to biochemical changes characteristic of biological aging and many pathological conditions, including diabetes, atherosclerosis and Alzheimer's disease [1–3]. A number of recent studies have focused on nuclear proteins as targets for non-enzymic modifications, which could have important implications for the maintenance of genomic integrity. For example, age-dependent increases in deamidation of histone H1° occur *in vivo* [4] and exposure of histone H1 to ionizing radiation generates protein-bound hydroperoxides that can give rise to free radicals, which damage DNA [5].

Protein carbonylation represents non-enzymic damage that can result by a number of different pathways. Protein-bound carbonyl groups are generated by direct oxidation of amino acid residues, such as lysine and arginine, by reaction with aldehydes, such as 4-hydroxy-2-nonenal and malondialdehyde, produced by lipid peroxidation, and as a result of reaction with reducing sugars or their oxidation products [3,6,7]. The reaction with reducing sugars can generate protein carbonyls as ketoamines derived from early glycation reactions and by more complex glycoxidation reactions that lead to the generation of fluorescent advanced glycation end products (AGEs) and protein cross-links [3,8,9]. The presence of nuclear protein carbonyls has been detected *in vivo* [10], but specific protein targets have not yet been identified. The detection of a nuclear proteasome that degrades histones oxidized *in vitro* [11] also suggests that nuclear protein carbonylation probably has physiological relevance. The possibility that specific nuclear proteins may be targets for protein carbonylation by glycation is supported by reports of accumulation of AGEs on liver histones of streptozotocin-induced diabetic rats [12] and glycation of high mobility group (HMG) proteins in calf thymus [13].

To further elucidate the biological significance of intranuclear protein carbonylation, we studied histone carbonylation *in vivo* and *in vitro*. In the present study we report the identification of histone H1 as a preferential carbonylation target *in vivo*. We demonstrate the accumulation of carbonylated histones in rat pheochromocytoma cells (PC12 cells) following alkylating stress. Finally, we describe one possible mechanism of histone carbonylation using PC12 nuclei and isolated histone H1 as glycation targets.

MATERIALS AND METHODS

Chemicals

NaB^3H_4 (radiolabelled sodium borohydride) was obtained from NEN Life Science Products (Boston, MA, U.S.A.). All other chemicals were purchased from Sigma Chemical Co. Calf tissues (thymus, liver and spleen), frozen in liquid nitrogen immediately after collection, were from Pel-Freez Biologicals (Rogers, AR, U.S.A.).

Preparation of AGE-BSA

AGE-BSA was prepared as described by Takata et al. [14]. Briefly, 1.6 g of BSA was dissolved with 3 g of D-glucose in 10 ml of 0.5 M sodium phosphate buffer (pH 7.4), containing 0.05 % NaN_3. The solution was filter-sterilized through a 0.45 μm filter and incubated in the dark for 90 days at 37 °C. Following dialysis against water, the sample was freeze-dried.

Large-scale isolation of histone H1 from calf thymus

All operations were carried out at 4 °C. Chromatin was isolated from calf thymus by extraction with 0.14 M NaCl/0.05 M $Na_2S_2O_5$ (pH 5.0), as described by Johns [15]. After repeated extraction with 5 % (w/v) $HClO_4$ and centrifugation at 1500 ***g*** for 30 min, histone H1 was precipitated by addition of trichloroacetic acid (TCA) to a final concentration of 20 % (w/v).

Abbreviations used: AGEs, advanced glycation end products; DNPH, 2,4-dinitrophenylhydrazine; DTPA, diethylenetriaminepentaacetic acid; HMG, high mobility group; MALDI–FT-MS, matrix-assisted laser-desorption ionization–Fourier-transformed-MS; MNNG, *N*-methyl-*N*′-nitro-*N*-nitrosoguanidine; PC12 cells, rat pheochromocytoma cells; RP, reverse-phased; TCA, trichloroacetic acid.

[1] To whom correspondence should be addressed (e-mail mjacob1@pop.uky.edu).

The histone H1 precipitate was collected by centrifugation at 12000 ***g*** for 30 min and resuspended in water. After dialysis (molecular-mass cut-off, 12000–14000 Da) against water for 48 h the sample was freeze-dried and stored at 4 °C. SDS/PAGE (12 % polyacrylamide) was used to analyse the purity of the preparation.

Isolation of histone H1, core histones and total histones from calf tissues

Frozen bovine tissue (3 g) was ground on ice using a mortar and a pestle. First, intact nuclei were prepared according to a standard procedure [16]. The ground tissue was homogenized in 20 ml of ice-cold 10 mM Tris/HCl (pH 7.4), 10 mM NaCl, 3 mM $MgCl_2$, 0.5 % Nonidet P40 and 1 mM PMSF (solution A) using a Dounce homogenizer. Cell breakage was monitored by microscopy after staining the sample with 0.5 % Trypan Blue. An aliquot (5 ml) of the cell lysate was layered on to a 5 ml cushion of solution B [30 % (w/v) sucrose in solution A] and nuclei were pelleted by centrifugation at 2000 ***g*** for 5 min at 4 °C. For the preparation of histone H1, the nuclear pellet was first extracted two times with three volumes of 5 % (w/v) $HClO_4$ for 30 min on ice with occasional vortex-mixing. $HClO_4$-insoluble material was subsequently removed by centrifugation at 15000 ***g*** for 15 min, and soluble proteins were precipitated by adding ice-cold TCA to a final concentration of 20 % (w/v). After 10 min on ice, the precipitated protein was recovered by centrifugation at 15000 ***g*** for 15 min and the pellet was washed with diethyl ether. The protein was dissolved in water and was further purified by microdialysis against water at 4 °C. To prepare core histones, the $HClO_4$-insoluble material was extracted two times with three volumes of 0.2 M H_2SO_4 for 10 min on ice, and further processed as indicated above. For preparation of total histones, the nuclear pellet was directly extracted with 0.2 M H_2SO_4.

For comparative purposes, histone H1 was also prepared by extracting the nuclear pellet with 0.5 M NaCl, and core histones were prepared by subsequent extraction of the residual nuclear pellet with 2 M NaCl, as described previously [17]. Additionally, total histones were extracted with one volume of 12 % (w/v) SDS after suspending the nuclear pellet in a stabilizing buffer containing 5 mM Tris/HCl (pH 7.4), 2.5 mM KCl and 5 mM $MgCl_2$ (TKM buffer), and incubating with 0.1 unit/μl DNase I and 25 μg/ml RNase A for 5 min at 37 °C.

Pretreatment and isolation of intact nuclei from PC12 cells

PC12 cells were grown, in Dulbecco's modified Eagle's medium containing 5 % (v/v) fetal calf serum and 10 % (v/v) horse serum, to high density in T-75 flasks. After treatment with H_2O_2 or *N*-methyl-*N*′-nitro-*N*-nitrosoguanidine (MNNG) as indicated in Figure 3, the cells were removed from the flasks by trypsin treatment, and collected by centrifugation. Intact nuclei were prepared according to a standard procedure [16]. The nuclear pellet was suspended in TKM buffer and kept on ice.

Incubation of intact nuclei with ADP-ribose or D-glucose, and extraction of total histones

Intact nuclei (20 μl) were resuspended in 200 μl of TKM buffer containing 2 mM ADP-ribose or 2 mM D-glucose, and incubated for 2 h at 37 °C. After centrifugation, the nuclear pellet was washed with TKM buffer and extracted with 300 μl of 0.2 M H_2SO_4 for 10 min on ice. After centrifugation at 15000 ***g*** for 15 min, 75 μl of ice-cold 100 % (w/v) TCA was added to the supernatant. After 10 min on ice, the precipitated protein was recovered by centrifugation at 15000 ***g*** for 15 min and the pellet was washed with diethyl ether. The histones were re-dissolved in water and immediately incubated with 2,4-dinitrophenylhydrazine (DNPH).

Oxidative modification of histone H1

Oxidative modification of histone H1 for carbonylation analysis was performed according to Chao et al. with slight modifications [18]. Histone H1 (1 mg/ml) was incubated in physiological PBS containing 100 μM $FeSO_4$, 25 mM ascorbate and 25 mM H_2O_2 at 37 °C for 4 h The reagents were removed by microdialysis (MEGA System Microdialyzer; molecular-mass cut-off, 12000–14000 Da; Health Products, Rockford, IL, U.S.A.) and an aliquot of the protein solution was used for further analysis.

Glycation of histone H1 or BSA by ADP-ribose at physiological pH

Incubations of 1.0 ml contained 50 mM potassium phosphate (pH 7.4), 1.0 mM ADP-ribose, 1.5 mg of histone H1 or BSA, and 0.015 % NaN_3. Incubations were carried out at 37 °C in the dark. Incubations at pH 9.0 were performed as reported previously [19]. When present, transition metal ion chelators EDTA, diethylenetriaminepentaacetic acid (DTPA), and other reagents were added from concentrated solutions in phosphate buffer. Oxygen was excluded from the reaction mixtures by bubbling with argon gas for 5 min and then sealing reaction vessels under a stream of argon. Reaction aliquots of 100 μl were dialysed against distilled water using a microdialysis system.

Immunodetection of protein-bound carbonyl groups

Derivatization of protein-bound carbonyl groups with DNPH and immunodetection were performed according to the procedure of Shacter et al. [20]. Briefly, 5 μl of 12 % SDS was added to a 5 μl aliquot of sample containing 5 μg of protein. After addition of 10 μl of 10 mM DNPH in 10 % (v/v) trifluoroacetic acid, the mixture was incubated for 20 min at room temperature. The reaction mixture was neutralized and prepared for SDS/PAGE by adding 7.5 μl of 2 M Tris base containing 30 % (v/v) glycerol. Proteins were separated by SDS/PAGE and transferred on to a nitrocellulose membrane using a semi-dry system. A second gel containing duplicate samples was run and stained with Coomassie Blue. Additionally, equal transfer was checked by reversible protein staining of the nitrocellulose membrane with Ponceau S. The anti-DNP antibody (V401) was supplied by DAKO (Carpinteria, CA, U.S.A.) and used at 1:1000 dilution. The secondary antibody was goat anti-rabbit conjugated with horseradish peroxidase (Jackson Immunoresearch Laboratories, Bar Harbor, ME, U.S.A.) used at 1:20000 dilution. Immunoblots were visualized using ECL® detection reagents supplied by Amersham, with exposure times between 5 s and 3 min.

Immunodetection of histone H1

Histone H1 was identified on the same nitrocellulose membranes previously used for immunodetection of protein-bound carbonyl groups. Anti-(histone H1) serum from sheep was supplied by Maine Biotechnology Services (Portland, ME, U.S.A.), and was used at 1:200 dilution. The secondary antibody was donkey anti-sheep IgG conjugated with horseradish peroxidase from Sigma, and was used at 1:5000 dilution. Immunoblots were visualized using ECL® detection reagents.

Reductive tritium incorporation into glycated and oxidized proteins

Protein-bound carbonyl groups were reduced and quantified by the method of Lenz et al. [21]. All determinations were performed in triplicate. Briefly, an aliquot containing 200–600 μg of protein was dissolved in 50 μl of water followed by addition of 6 μl of 1 M Tris/HCl (pH 8.5)/10 mM EDTA and 14 μL of NaB^3H_4 in 0.1 M NaOH (specific activity, 100 mCi/mmol). After incubation at 37 °C for 30 min, 330 μl of water was added, the sample was cooled on ice, and 100 μl of ice-cold 100 % TCA was added. After 10 min on ice, the sample was centrifuged at 11000 ***g*** for 15 min and the precipitate was washed with ice-cold 20 % TCA and diethyl ether. The pellet was re-dissolved in 10–20 μl of 12 % SDS and diluted with water to a final concentration of less than 1 % SDS. After centrifugation at 11000 ***g*** for 15 min, protein was quantified using the bicinchoninic acid-reaction kit from Pierce (Rockford, IL, U.S.A.). Scintillation cocktail (5 ml of EcoLume from ICN; Costa Mesa, CA, U.S.A.) was added and radioactivity was determined by liquid scintillation counting on a Beckman LS 6500 counter.

Preparation and derivatization of N^{α}-acetyl-N^{ε}-(1′′-deoxy-ADP-ribulos-1′′-yl)-L-lysine

A 100 μl reaction mixture containing 50 mM potassium phosphate (pH 7.4), 10 mM ADP-ribose and 1.0 M N^{α}-acetyl-L-lysine, was incubated for 24 h at room temperature, and samples were analysed periodically by reversed-phase (RP)-HPLC. The reduced ketoamine was prepared by addition of 6 μl of 1 M Tris (pH 8.5)/10 mM EDTA and 14 μl of 200 mM $NaBH_4$ in 0.1 M NaOH to 50 μl of the above reaction mixture. After incubation at 37 °C for 30 min, the mixture was acidified with HCl, mixed, and neutralized with NaOH. The oxime derivative of the ketoamine was prepared by incubation of the ketoamine with 1 M hydroxylamine for 1 h at 37 °C. All reaction products were purified by preparative RP-HPLC for analysis by NMR and MS. RP-HPLC used a μBondapak C_{18} column (3.9 mm × 300 mm) from Waters (Milford, MA, U.S.A.) with a gradient elution. Running solution A was 50 mM ammonium formate (pH 5.0) and running solution B was 100 % methanol. The concentration of methanol was 0 % for 15 min, 0–5 % from 15–20 min, and 5 % from 20–40 min. The eluate was monitored at 254 nm. MS was performed using IonSpec HiRes MALDI–Fourier-transformed-MS (MALDI–FT-MS). Spectra were recorded with high resolution in negative ion mode after dissolving samples in H_2O/methanol (1:1, v/v). The matrix used was 2,5-dihydroxybenzoic acid.

RESULTS

Metal-catalysed oxidation and glycation of histone H1 results in the introduction of protein carbonyl groups

It is known that oxidation and glycation lead to the formation of carbonyl groups on target proteins [3,8,9]. Proteins modified by carbonyl groups due to oxidative modifications can be detected by immunoassay following derivatization with the carbonyl-specific reagent DNPH [20]. We examined the feasibility of using this approach to detect protein damage on histone H1 after metal-catalysed oxidation or glycation by ADP-ribose. ADP-ribose is a reducing sugar generated in the nucleus in proportion to DNA strand breaks following genotoxic stress [22–24]. Figure 1 shows SDS/PAGE analysis of histone H1 stained by Coomassie Blue (Figure 1A) and immunostained for protein-bound DNP epitopes (Figure 1B), following various treatments. BSA incubated for 90 days with 1.66 M D-glucose (AGE-BSA) served as a reference standard for the introduction of carbonyl groups by glycation [14]. The AGE-BSA readily displayed carbonyl-specific epitopes on both monomeric and cross-linked forms of the protein (lane 2). As little as 10 ng of AGE-BSA was readily detectable by carbonyl immunostaining. As reference standards for the direct introduction of carbonyl groups by oxidative mechanisms, histone H1 was incubated with H_2O_2 alone or in the presence of ascorbate and $FeSO_4$ to establish conditions for the Fenton reaction. Incubation with 25 mM H_2O_2 alone at pH 7.4 did not result in detectable carbonyl immunostaining (lane 4), but inclusion of ascorbate and $FeSO_4$ along with H_2O_2 resulted in strong immunostaining indicating extensive protein carbonylation and protein degradation (lane 5). Strong carbonyl immunostaining of both the monomer and cross-linked forms of histone H1 (lane 6) was detected. This finding is consistent with our previous observations that incubation of histone H1 in the presence of ADP-ribose at pH 9.0 results in extensive protein cross-linking [19]. The immunostaining of this sample was dependent upon reaction with DNPH since immunostaining was completely eliminated when DPNH was omitted (lane 7). Incubation of histone H1 for 7 days with 1 mM ADP-ribose at pH 7.4 resulted in strong carbonyl immunostaining (lane 9). Detectable immunostaining of the histone H1 monomer occurred after incubation at pH 7.4 for only 2 h (lane 8). Interestingly, upon prolonged exposure of the film, untreated histone H1 (lane 3) displayed detectable carbonyl immunostaining, whereas equal amounts of untreated BSA (lane 1) or core histones did not (results not shown). This suggested that histone H1 may have a significant background level of carbonylation *in vivo*.

The results of Figure 1 indicated that carbonyl-specific immunostaining would be useful for the characterization of damage to histone H1 by oxidation and/or glycation. We quantified the amount of protein-bound carbonyls after oxidation or glycation with ADP-ribose by reductive tritium incorporation, from NaB^3H_4, into the target protein according to a standard procedure [21]. The results are shown in Table 1. Proteins not incubated or incubated in the absence of D-glucose or ADP-ribose incorporated very low levels of radiolabel. However, untreated histone H1 displayed nearly 3-fold higher levels of incorporation than untreated BSA (nmol carbonyl/mg protein) again indicating the presence of a small but significant amount of protein-bound carbonyl groups on histone H1 *in vivo*. Pre-reduction of the histone H1 sample with $NaBH_4$ reduced the incorporation of radiolabel on histone H1 by 4-fold indicating that incorporation of radiolabel was not due to non-specific incorporation (results not shown). Again, AGE-BSA served as reference standard and nearly 100 nmol of carbonyl groups per mg of protein were detected. Consistent with the results observed by carbonyl-immunostaining (Figure 1) incubation of histone H1 with H_2O_2 alone resulted in barely-detectable formation of carbonyl groups, while Fenton reaction conditions resulted in the formation of more than 80 nmol of carbonyl groups per mg of histone H1. Incubation of histone H1 with ADP-ribose at pH 7.4 for 1 or 7 days resulted in the formation of 25.1 and 38.7 nmol of carbonyl groups per mg of protein respectively. The amount of modification by ADP-ribose in 1 day at pH 7.4 was approximately 50 % of that observed following incubation for 1 day at alkaline pH, which is known to accelerate the reaction [19]. On a molar basis, incubation with ADP-ribose produced 1 mol of carbonyl group per mol of histone H1 protein, even at pH 7.4. The quantification reported in Table 1 is in good agreement with the intensity of the carbonyl immunostaining shown in Figure 1, indicating that the immunostaining reflects the relative levels of protein modification by carbonyl groups.

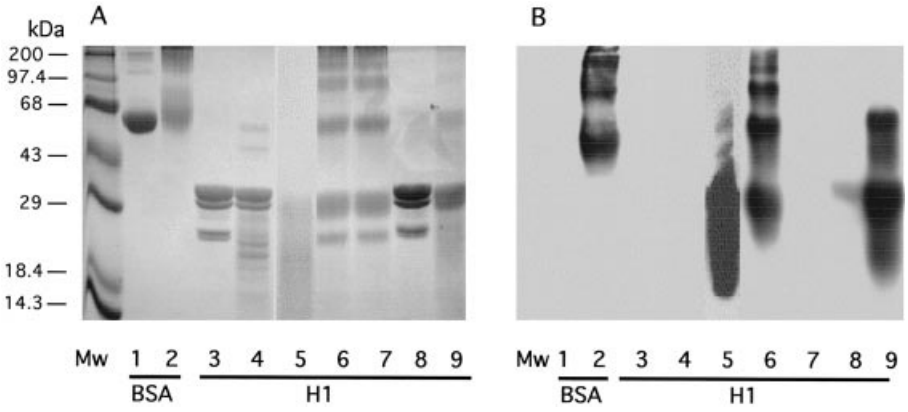

Figure 1 Carbonylation of BSA and histone H1: detection by carbonyl immunostaining

Protein samples [4 μg in (**A**) and 1 μg in (**B**)] were analysed by SDS/PAGE (12% polyacrylamide) with Coomassie staining (**A**) or after DNPH-derivatization and transfer on to nitrocellulose with carbonyl immunostaining (**B**). Lanes 1 and 2 contained BSA incubated for 90 days at pH 7.4 without sugar (lane 1) or in the presence of 1.66 M D-glucose (lane 2). Lanes 3–9 contained histone H1 incubated for 1 day at pH 7.4 with no additions (lane 3), for 2 h at pH 7.4 with 25 mM H_2O_2 (lane 4), or for 4 h at pH 7.4 with 25 mM H_2O_2, 25 mM ascorbate and 100 μM $FeSO_4$ (lane 5). Lanes 6–9 contained 1 mM ADP-ribose incubated for 1 day at pH 9.0 (lane 6), as in lane 6 except that DNPH was omitted from the procedure (lane 7), at pH 7.4 for 2 h (lane 8) or at pH 7.4 for 7 days (lane 9).

Table 1 ^{3}H-incorporation into BSA and histone H1 after reaction with various agents: quantification of protein-bound carbonyls

Protein samples (200–600 μg) were reacted with $NaBT_4$ and tritium incorporation was quantified as described in the Materials and methods section. Data are given as the means ± S.D. ($n = 3$). The metal-catalysed oxidation (MCO) system contained 25 mM H_2O_2, 25 mM ascorbate and 100 μM $FeSO_4$.

					Protein bound carbonyls	
Protein	Compound (concentration)	Reaction time	pH	^{3}H-incorporation (c.p.m./μg of protein)	(nmol carbonyl/mg of protein)	(mol of carbonyl/mol of protein)
BSA	None	–	–	100 ± 12	1.5 ± 0.2	0.10 ± 0.01
BSA	None	7 days	7.4	111 ± 10	1.7 ± 0.2	0.11 ± 0.01
BSA	Glucose (1.66 M)	90 days	7.4	6610 ± 1040	100 ± 15.8	6.81 ± 1.08
H1	None	–	–	254 ± 7	3.9 ± 0.1	0.08 ± 0.00
H1	None	7 days	7.4	259 ± 31	3.9 ± 0.5	0.08 ± 0.01
H1	ADP-ribose (1 mM)	1 days	7.4	1910 ± 130	29.0 ± 2.0	0.61 ± 0.04
H1	ADP-ribose (1 mM)	7 days	7.4	2810 ± 120	42.6 ± 1.8	0.89 ± 0.04
H1	ADP-ribose (1 mM)	1 days	9.0	3410 ± 180	51.7 ± 2.7	1.09 ± 0.06
H1	H_2O_2 (25 mM)	2 h	7.4	308 ± 55	4.7 ± 0.8	0.10 ± 0.02
H1	MCO	4 h	7.4	5600 ± 510	84.9 ± 7.8	1.78 ± 0.16

Background levels of protein-bound carbonyl groups on histone H1 and other nuclear proteins in mammalian tissues

Our detection of significant carbonylation of untreated histone H1 led us to further investigate the carbonyl background levels on histone extracted from bovine tissue. Extracted histones were analysed by SDS/PAGE followed by Coomassie Blue staining and carbonyl immunostaining (Figure 2). Carbonyl immunostaining demonstrated that the histone H1-fractions extracted from bovine thymus, liver and spleen contained significantly elevated amounts of protein-bound carbonyl groups compared to the core histone-fractions (Figure 2B). This difference was most pronounced in the thymus, but was also apparent in the liver and the spleen. This pattern of histone carbonylation was seen with several different batches of bovine tissue. Consistent with the patterns observed in the immunoblots, reductive tritium incorporation into the histone H1-fraction from thymus was 7-fold greater than the incorporation into core histones (3.90 nmol/mg of histone H1 compared with 0.56 nmol/mg of core histone). As a control for artifactual introduction of carbonyl groups during preparation of histone H1, samples containing total histones were also examined. In these samples only histone H1 showed appreciable carbonyl immunostaining. Interestingly, in histone H1-fractions, two additional protein bands migrating with apparent molecular-masses slightly below 29 kDa showed strong carbonyl immunostaining (as indicated by the arrowheads in Figures 2A and 2B). Based on apparent molecular size and extraction characteristics, these proteins are most probably HMG1/2, members of the basic HMG nuclear proteins [13]. These proteins are typically contaminants in histone H1 preparations obtained by perchloric acid- or NaCl-extraction of nuclei [13]. To further exclude the artifactual introduction or destruction of protein carbonyl groups during histone preparation and analysis, several control experiments were performed (Figures 2C and 2D). Alternative methods of histone preparation, involving extraction of total histone into 12% SDS or sequential salt extraction of histone H1 and core histones, gave the same results for carbonyl immunostaining as shown in Figure 2 (results

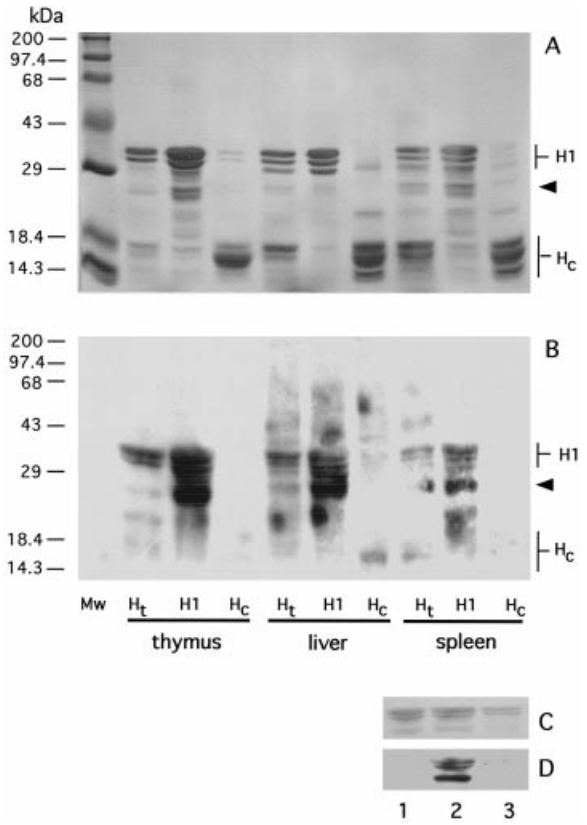

Figure 2 Increased levels of carbonylation on histone H1 in bovine tissues

Total histone (H_t), histone H1 (H1), and core histones (H_c) were prepared from fresh nuclei from bovine tissues (thymus, liver and spleen) as described in the Materials and methods section. Protein samples [5 μg in (**A**) and 2 μg in (**B**)] were analysed by SDS/PAGE (15% polyacrylamide) with Coomassie staining (**A**) or after DNPH-derivatization and transfer on to nitrocellulose with carbonyl immunostaining (**B**). As a control (**C**: Ponceau stain; **D**: carbonyl immunostaining), histone H1 fractions were processed as above, but in the presence (lane 2) or absence of DNPH (lane 1), and after pre-reduction with $NaBH_4$ (lane 3). The arrowheads indicate the position of other nuclear proteins with high carbonyl immunostaining, presumably HMG1/2.

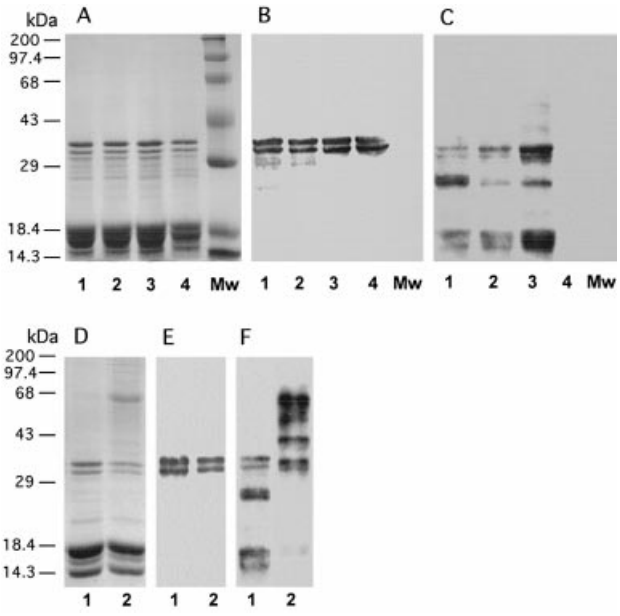

Figure 3 Histone carbonylation in PC12 cells under oxidative and alkylating stress

PC12 cells grown to high density in T-75 flasks were sham-treated (**A**–**C**, lane 1) or exposed to H_2O_2 (2 mM) added to the medium for 1 h (**A**–**C**, lane 2). Another group of cells was exposed to H_2O_2 (2 mM), added to the medium for 1 h and MNNG (20 μg/ml) was added for the last 20 min (**A**–**C**, lane 3). In another set of experiments, PC12 cells were sham-treated (**D**–**F**, lane 1) or exposed to MNNG (20 μg/ml), added to the medium for 1 h (**D**–**F**, lane 2). After preparation of the nuclei, total histones were extracted with 0.2 M H_2SO_4. Protein samples [8 μg in (**A**) and (**D**); 2 μg in (**B**), (**C**), (**E**) and (**F**)] were analysed by SDS/PAGE (15% polyacrylamide) with Coomassie staining (**A** and **D**) or after DNPH-derivatization transferred on to nitrocellulose with carbonyl immunostaining (**C** and **F**) and subsequent immunostaining for histone H1 (**B** and **E**). As a control, a duplicate sample as in (**A**–**C**, lane 3) was processed without DNPH (**A**–**C**, lane 4).

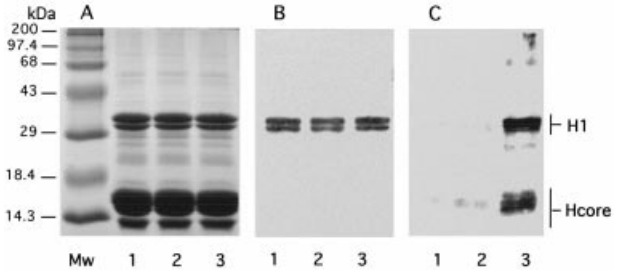

Figure 4 Carbonylation of histones by ADP-ribose in intact mammalian nuclei

Intact nuclei from PC12 cells (50 μl) were incubated with 2 mM D-glucose or 2 mM ADP-ribose at pH 7.4 in TKM buffer at 37 °C for 2 h Total histones were extracted and equal aliquots (8 μg) were analysed by SDS/PAGE (15% polyacrylamide) with subsequent Coomassie staining (**A**). Another aliquot (2 μg) was reacted with DNPH and, following SDS/PAGE, was transferred on to a nitrocellulose membrane and analysed by carbonyl immunostaining (**C**) and subsequent immunostaining for histone H1 (**B**). Lane 1 shows an incubation without added sugar, lane 2 shows addition of D-glucose and lane 3 shows addition of ADP-ribose. The migration positions of histone H1 (H1) and core histones (Hcore) are indicated on the right.

not shown). Omission of DNPH during the derivatization step of the histone H1 fraction (Figure 2D, lane 1) or pre-reduction of this fraction with $NaBH_4$ (Figure 2D, lane 3) eliminated the carbonyl immunostaining displayed by the complete reaction mixture (Figure 2D, lane 2).

Stress-induced histone carbonylation in cultured mammalian cells

PC12 cells, a widely used model for the study of oxidative damage in mammalian neuronal-like cells [25], were used to investigate histone carbonylation following oxidative and alkylating stress (Figure 3). Exposure to H_2O_2 (2 mM) was chosen as an oxidative stress [11], and exposure to the alkylating agent MNNG (20 μg/ml), known to induce DNA strand breaks and rapid ADP-ribose polymer synthesis and turnover [22], was chosen as an alkylating stress. Following treatment, nuclei were isolated, histones were extracted and analysed by SDS/PAGE, followed by Coomassie Blue staining, histone H1 immunostaining and carbonyl immunostaining. Samples from control cells showed background carbonyl immunostaining that was especially pronounced in the HMG1/2-region of the gel (Figure 3C, lane 1 and Figure 3F, lane 1). Treatment with H_2O_2 induced only a modest increase of carbonylation of the upper histone H1 band (Figure 3C, lane 2), but a considerable decrease of carbonylation in the HMG1/2 region of the gel, most probably indicating a rapid turnover of this material in response to

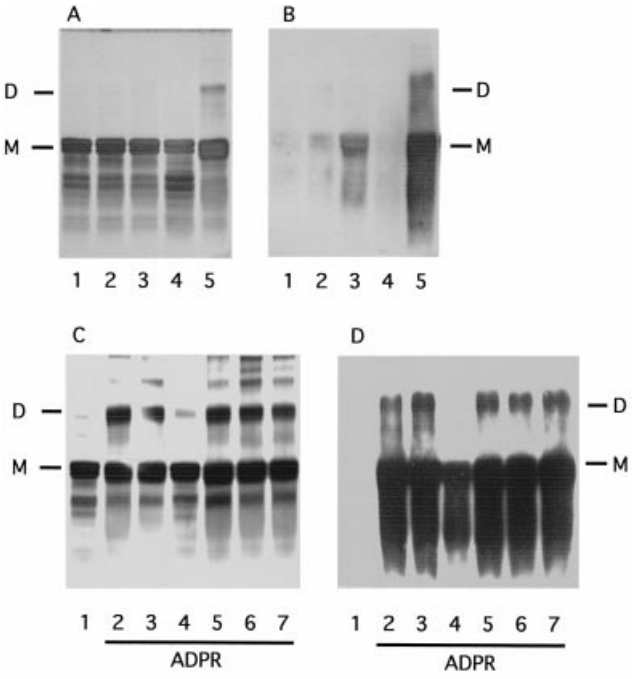

Figure 5 Comparative glycation of histone H1 by different sugars and effects of antioxidant conditions and reagents on protein cross-linking and carbonylation

(**A** and **B**) Reaction mixtures containing histone H1 and 1 mM of different sugars were incubated at pH 7.4. At day 7, reaction aliquots were analysed by SDS/PAGE (12% polyacrylamide) with subsequent silver staining (**A**) or carbonyl immunostaining (**B**). Lane 1 shows a control reaction with no added sugar and the sugars present in the other lanes were D-glucose (lane 2), D-ribose (lane 3), ADP-glucose (lane 4), and ADP-ribose (lane 5). (**C** and **D**) Reaction mixtures containing histone H1, 1.0 mM ADP-ribose, and other additions were incubated at pH 7.4. At day 7, aliquots were analysed by SDS/PAGE (12% polyacrylamide) with subsequent silver staining (**C**) and carbonyl immunostaining (**D**). Lane 1 shows a reaction without added ADP-ribose. Lanes 2–7 show reactions with ADP-ribose and no other additions (lane 2), addition of 5 mM DTPA under argon (lane 3), 5 mM aminoguanidine (lane 4), 5 mM N^{α}-acetyl-L-cysteine (lane 5), 5 mM mannitol (lane 6), or 100 units/ml of catalase (lane 7). M and D refer to the migration position of histone H1 monomer and dimer respectively.

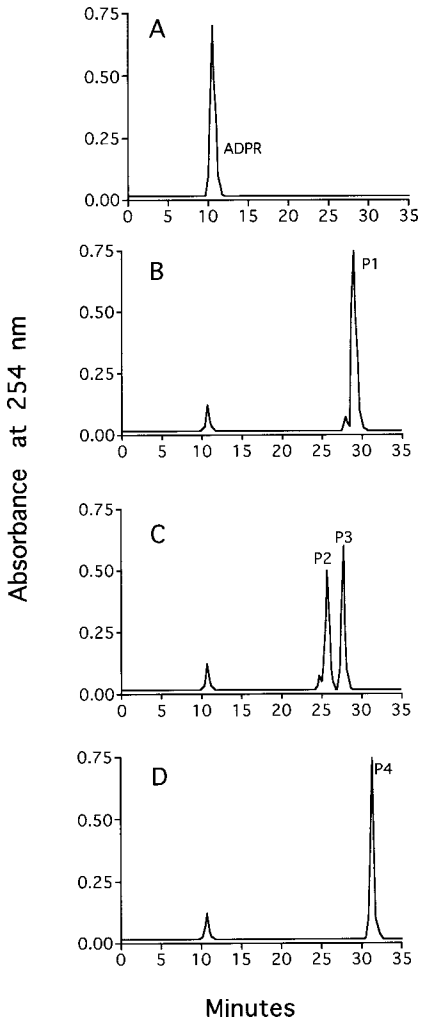

Figure 6 Reaction of N^{α}-acetyl-L-lysine with ADP-ribose at pH 7.4

A reaction containing 1 M N^{α}-acetyl-L-lysine was incubated with 10 mM ADP-ribose in 50 mM potassium phosphate buffer (pH 7.4). A reaction aliquot was analysed by RP-HPLC, with UV detection at 254 nm at zero time (**A**) and after 24 h (**B**). At 24 h the reaction mixture was subjected to reduction by $NaBH_4$ (**C**). The isolated reaction product P1 was incubated with hydroxylamine before RP-HPLC analysis (**D**). The positions of ADP-ribose (ADPR) and reaction products P1–P4 are indicated.

oxidative stress. Treatment with MNNG resulted in less protein in the histone H1 band (Figures 3D and 3E, lanes 2), but increased carbonyl immunostaining of histone H1 (Figure 3F, lane 2). Remarkably, Coomassie stain (Figure 3D, lane 2) and carbonyl immunostaining (Figure 3F, lane 2) revealed new protein bands migrating at slightly less than 68 kDa, a region where histone H1 dimers would appear (Figure 1, lane 9). However, the histone H1 immunostaining could not confirm the identity of this heavily carbonylated protein as histone H1-dimer (Figure 3E, lane 2). When H_2O_2 was administered in combination with MNNG, strong carbonyl immunostaining of histone H1 and core histones was observed (Figure 3C, lane 3). Controls demonstrating the requirement for DNPH-derivatization for immunostaining (Figure 3C, lane 4) and ruling out non-specific protein binding during immunostaining (Figure 3C, lane 5) are also shown.

Histones in isolated mammalian nuclei are rapidly carbonylated by ADP-ribose

The modest effect of H_2O_2 treatment, the strong effects of MNNG treatment, and the synergistic effect of oxidative and alkylating stress on nuclear protein carbonylation in PC12 cells suggested that accumulation of histone carbonyl groups involves mechanisms in addition to direct oxidative introduction of carbonyl groups into nuclear proteins. Since MNNG-induced DNA damage is known to result in the intranuclear generation of the reducing sugar ADP-ribose [22,23], the possibility that the histone carbonylation was derived from glycation and/or glycoxidation reactions initiated by ADP-ribose was examined. Freshly prepared nuclei from PC12 cells were incubated for 2 h in a nuclear stabilization buffer at pH 7.4 containing 2 mM ADP-ribose or 2 mM D-glucose. Extracted proteins were analysed by SDS/PAGE followed by Coomassie Blue staining, histone H1 immunostaining and carbonyl immunoblotting (Figure 4). The presence of ADP-ribose resulted in strong carbonyl-specific immunostaining (Figure 4C, lane 3), while the presence of D-glucose resulted in barely-detectable immunostaining (Figure 4C, lane 2) and histones from a control incubation without added sugars did not show detectable immunostaining (Figure 4C, lane 1) at the chosen exposure time of the film. When ADP-

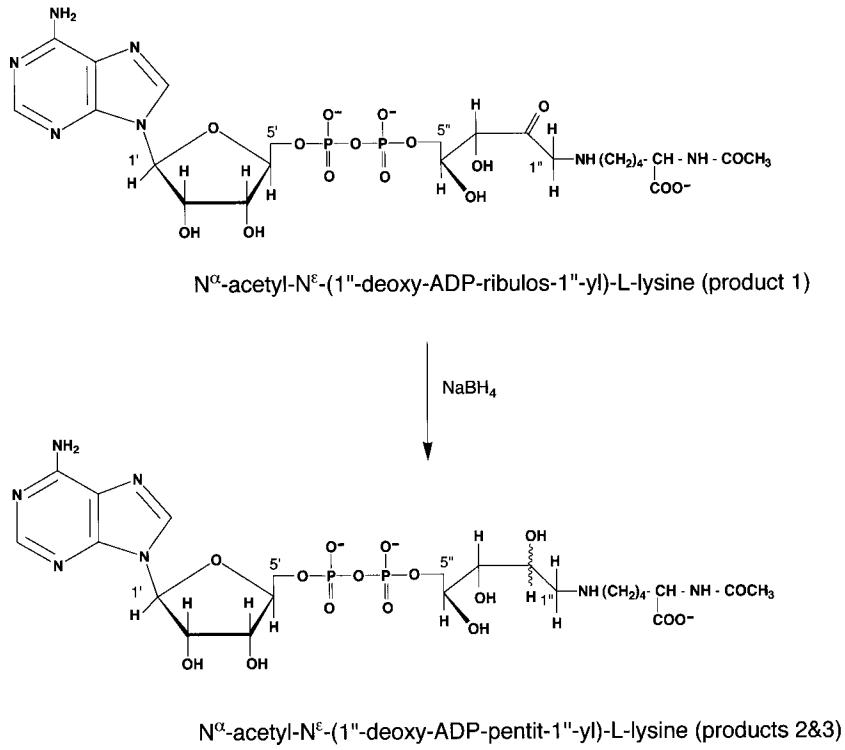

N^{α}-acetyl-N^{ε}-(1"-deoxy-ADP-ribulos-1"-yl)-L-lysine (product 1)

N^{α}-acetyl-N^{ε}-(1"-deoxy-ADP-pentit-1"-yl)-L-lysine (products 2&3)

Scheme 1 The ADP-ribose derived ketoamine and its epimeric reduction products

N^{α}-acetyl-L-lysine was reacted with ADP-ribose at pH 7.4, as described in the Materials and methods section. Treatment of the ketoamine (product 1) with $NaBH_4$ yielded two epimers (products 2 and 3).

ribose was used, the majority of carbonyl immunoreactivity was present in the histone H1 region, especially in the upper band as already observed in intact PC12 cells exposed to H_2O_2 and MNNG (Figure 3). Immunoreactivity also appeared in the region of the core histones with the exception of histone H4 (lowest band of core histones).

Carbonylation of histone H1 by ADP-ribose is more potent than by other sugars and does not involve oxidative pathways

Since ADP-ribose was much more potent than glucose in causing histone carbonylation in isolated nuclei, its carbonylation reactivity was compared with other reducing sugars in experiments in which sugars were incubated at pH 7.4 with histone H1 for an extended period (1 week) due to the low carbonylation activity of most of the sugars tested. As seen in Figure 5 ADP-ribose caused extensive carbonylation (Figure 5B, lane 5), D-ribose caused a lesser amount (Figure 5B, lane 3), and neither D-glucose (Figure 5B, lane 2) nor ADP-glucose (Figure 5B, lane 4) caused significant carbonylation, even at the extended incubation times used in this experiment. The amount of carbonylation caused by ADP-ribose (0.82 mole/mole of histone H1) and D-ribose (0.06 mole/mole of histone H1), determined by incorporation of NaB^3H_4, correlated with the relative amounts of immunostaining caused by these sugars.

To determine if the carbonylation of histone H1 by ADP-ribose involved oxidative reaction pathways, several compounds known to interfere with the glycoxidation of proteins by D-glucose [26] were examined for their effects on protein carbonylation by ADP-ribose (Figures 5C and 5D). Different reagents including the transition metal ion chelator DTPA in the absence of oxygen (lane 3), the nucleophilic antioxidant N^{α}-acetyl-L-cysteine (lane 5), the hydroxyl radical scavenger mannitol (lane 6), and the presence of catalase for the removal of traces of hydrogen peroxide (lane 7) did not interfere with histone carbonylation by ADP-ribose. Remarkably, only the dicarbonyl scavenger and inhibitor of advanced glycation, aminoguanidine [27], showed a slight inhibitory effect on carbonylation (Figure 5D, lane 4). In contrast, protein cross-linking was fully blocked. These data strongly suggest that histone H1 carbonylation by ADP-ribose at pH 7.4 is not a result of glycoxidation, but rather early glycation.

Structure elucidation of the carbonyl compound from early glycation by ADP-ribose

A model system designed to allow structural elucidation was developed to further characterize the nature of the carbonyl derivatives that rapidly accumulate on histone H1 during reaction with ADP-ribose at pH 7.4. N^{α}-acetyl-L-lysine, which imitates peptide-bound lysine as the most likely glycation target on histone H1, was reacted with ADP-ribose at pH 7.4. Reaction products were characterized by RP-HPLC as shown in Figure 6. Incubation for 24 h resulted in conversion of more than 90 % of the ADP-ribose into material termed P1, which migrated primarily as a single peak at approximately 29 min (Figures 6A and 6B). Although stable under the conditions of incubation and HPLC, P1 was partially degraded upon lyophilization and it was therefore derivatized for further analysis. Upon treatment with $NaBH_4$, P1 was quantitatively transformed into a mixture of two putative reduction products, termed P2 and P3, which migrated at approximately 26 and 27 min respectively (Figure 6C).

Treatment of P1 with hydroxylamine yielded material (P4) that migrated as a single peak at approximately 32 min (Figure 6D). MALDI–FT-MS of P2 and P3 material revealed a single $[M-H]^-$ of 730.190 Da, compatible with P2 and P3 representing a mixture of 2″-epimeric N^{α}-acetyl-N^{ϵ}-(1″-deoxy-ADP-pentit-1″-yl)-L-lysine ($C_{23}H_{39}N_7O_{16}P_2$, calculated $[M-H]^- = 730.195$ Da). Analysis of P4 revealed a single $[M\text{-}H]^-$ of 743.200 Da, compatible with the oxime of a ketoamine ($C_{23}H_{38}N_8O_{16}P_2$, calculated $[M-H]^- = 743.180$ Da) derived from ADP-ribose and N^{α}-acetyl-L-lysine. The proposed oxime structure for P4 was further validated by ^{13}C-NMR analysis that revealed a ^{13}C-signal (δ; 153.5 ppm) in the expected range of an oxime carbon (145–165 ppm) [28]. In addition to this signal, the expected signals for the five adenine carbon atoms (δ; 121.5 ppm, 142.4 ppm, 151.7 ppm, 154.5 ppm and 157.2 ppm) were observed (spectrum not shown). These chromatographic and spectroscopic data were in complete agreement with our previous analysis of the initial ketoamine product formed from the reaction of n-butylamine with ADP-ribose, where detailed ^{1}H-NMR analysis established the carbonyl group at position 2″ [29]. Taken together, the chromatographic and spectroscopic data indicate that the early glycation product (P1) is most probably the ketoamine N^{α}-acetyl-N^{ϵ}-(1″-deoxy-ADP-ribulos-1″-yl)-L-lysine that is converted to epimeric reduction products following treatment with $NaBH_4$ (Scheme 1). The ADP-ribose-derived ketoamine on histone H1 would be expected to react with DNPH because, in contrast to ketoamines originating from glycation by hexoses or other pentoses, the 5′-phosphate substitution of the D-ribose prevents stabilization by a closed ring hemiketal [8]. Prior studies have shown that DNPH readily forms hydrazones with the ketoamines derived from glyceraldehyde since this sugar is too short to cyclize [30]. Consistent with this suggestion, aminoguanidine, which effectively blocked advanced glycation, as assessed by protein crosslinking (Figures 5C and 5D), did not block the formation of the protein-bound carbonyl groups. Although aminoguanidine forms a hydrazone with ketoamines, the molar excess of DNPH during the derivatization reaction should displace most of the aminoguanidine. It is possible that the slight reduction in immunostaining of the histone H1 monomer observed in reactions containing aminoguanidine (Figure 5D, lane 4) may be the result of incomplete displacement by DNPH.

DISCUSSION

Protein carbonylation is elevated in pathological conditions and aging [1,3,7,31]. Histones are important potential targets for protein carbonylation due to their involvement in chromatin structure and function. Prior studies have detected protein-bound carbonyls in the nuclear fraction, although specific protein acceptors were not identified [10]. The present study has demonstrated, by two different methods, that histone H1 is one of the nuclear proteins modified by carbonyl groups *in vivo*. The immunological method for the detection of oxidized proteins, based on the derivatization of protein-bound carbonyl groups with DNPH and subsequent detection of the DNP-epitopes by immunoblotting [32], has led to the identification of a number of proteins that accumulate oxidative damage during the aging process [33]. The successful application of this method to detect histone carbonyl groups should facilitate the study of histone carbonylation under different physiological conditions.

The higher level of protein carbonylation in histone H1 relative to core histones is consistent with the higher accessibility of this linker histone as compared to core histones [34]. The carbonyl content of the histone H1 fraction from calf thymus (approximately 4 nmol of carbonyl/mg protein) as quantified by incorporation of radiolabel (Table 1) is similar to the reported levels of total protein-bound carbonyl groups in aged human dermal fibroblasts in tissue culture [35]. It will be interesting to examine the possibility that histone carbonylation increases with tissue age, as has been demonstrated for carbonyl content of total protein in different tissues [31]. The half-life of histones within non-proliferating mouse cells ranges between four and five months, potentially allowing the accumulation of non-enzymic histone damage with aging [36].

Our demonstration that histone carbonylation is increased following stress in PC12 cells must be interpreted in light of evidence that the nucleus contains a proteasome that preferentially degrades histones oxidized *in vitro* [11]. Thus the content of protein carbonyls obtained from cells or tissues probably reflects the relative rates of formation and degradation of proteins containing carbonyl groups. *In vitro*, H1 exhibited the highest rate of proteasomal degradation among histone fractions following oxidative damage by H_2O_2 [37]. Our detection of only slight increases in the accumulation of carbonylated H1 in PC12 cells following H_2O_2 treatment may only reflect efficient degradation of the oxidized H1 in these cells following oxidative stress. This possibility is supported by the decreased content of carbonyls in other nuclear proteins (the putative HMG1/2 samples) from H_2O_2-treated PC12 cells (Figure 3). Studies of the nuclear proteasome have shown that more highly oxidized histones containing cross-linked histone–DNA aggregates have decreased proteolytic susceptibility [37]. Thus it is possible that the histone carbonylation detected in our studies following alkylating stress or combinations of alkylating and oxidative stress may be due to the accumulation of protein damage that is not recognized, or poorly recognized, by the proteasome.

Since protein carbonylation involves a complex chemistry that can result in formation of carbonyls by multiple pathways, more studies will be required to identify the source(s) of histone carbonyl groups *in vivo*. One pathway that seems likely to account for histone carbonylation following alkylating stress is histone glycation. Monofunctional alkylating agents. like MNNG, are potent inducers of DNA strand cleavage, which activates the nuclear enzymes poly(ADP-ribose) polymerase and poly(ADP-ribose) glycohydrolase. The co-ordinated activities of these two enzymes results in the conversion of a large fraction of the millimolar-range NAD pool within minutes to free ADP-ribose in close proximity to basic histones [22,23]. The possibility that histone carbonylation *in vivo* is the result at least in part of glycation is supported by earlier studies by Hilz and co-workers that described ADP-ribose conjugates of histone H1 in hepatoma cells following alkylating stress [38] with chemical stability similar to histone glycation conjugates [29].

Although the involvement of free ADP-ribose in histone carbonylation *in vivo* is hypothetical at this point, several results reported in the present study support that possibility: (1) ADP-ribose readily results in the rapid introduction of carbonyls into H1 at physiological pH (Figure 1); (2) ADP-ribose is considerably more potent than other sugars examined in the introduction of carbonyls into H1 (Figure 5); (3) ADP-ribose causes carbonylation of histones in nuclei isolated from PC12 cells (Figure 4); (4) H1 was the dominant histone target for carbonylation by ADP-ribose in nuclei, a pattern reminiscent of that in tissues and cells (Figures 2 and 3). As to the nature of the carbonyl groups generated from ADP-ribose, the carbonylation of histone H1 by ADP-ribose *in vitro* during early glycation via oxygen-independent pathways (Figure 5) and the rapid conversion of ADP-ribose and N^{α}-acetyl-L-lysine at physiological pH into a ketoamine product (Figure 6 and Scheme 1) supports the

conclusion that an acyclic ketoamine is the primary source of protein-bound carbonyl groups derived from ADP-ribose. The ketoamine or its stabilized reduction product may be a useful biomarker for assessing the relevance of ADP-ribose induced carbonylation *in vivo*.

Enzymic post-translational modifications of histones that include methylation, acetylation, ubiquitination, poly(ADP-ribosyl)ation and phosphorylation are involved in the regulation of multiple chromatin functions [39]. Thus it is plausible that histone carbonylation may alter chromatin function. It has been reported that nucleosomal histone protein protects DNA from iron-mediated damage [40]. Nuclear polyamines like spermine are effective antioxidants protecting DNA from attack by reactive oxygen species, and a spermine-carbonyl adduct has been identified as a result of this function [41]. In an analogous manner, preferential histone carbonylation could serve to protect the chemical integrity of DNA. On the other hand, oxidative DNA damage has been demonstrated as a result of the decay of histone H1-bound hydroperoxides *in vitro*, suggesting a deleterious effect of oxidized histones on genomic integrity [5]. The methodology and results described in the present study should prove useful in investigating the functional significance of intranuclear protein carbonylation.

This research was supported by grants from the National Institutes of Health (CA43894 and NS38496) and Niadyne Inc. (University of Kentucky, Lexington, KY, U.S.A.). M. K. J. and E. L. J. are co-founders of Niadyne Inc., whose sponsored research is managed in accordance with the University of Kentucky conflict-of-interest policies. The assistance of Kristi Ballard with cell culture is gratefully acknowledged. Mass spectral analyses were performed by the University of Kentucky Mass Spectrometry Facility directed by Dr Jan Pyrek.

REFERENCES

1 Halliwell, B. and Gutteridge, J. M. C. (1989) Free radicals, ageing, and disease. In Free Radicals in Biology and Medicine, pp. 279–313, Clarendon Press, Oxford
2 Brownlee, M. (1995) Advanced protein glycosylation in diabetes and aging. Annu. Rev. Med. **46**, 223–234
3 Berlett, B. S. and Stadtman, E. R. (1997) Protein oxidation in aging, disease, and oxidative stress. J. Biol. Chem. **272**, 20313–20316
4 Lindner, H., Sarg, B., Hoertnagl, B. and Helliger, W. (1998) The microheterogeneity of the mammalian H1(0) histone. Evidence for an age-dependent deamidation. J. Biol. Chem. **273**, 13324–13330
5 Luxford, C., Morin, B., Dean, R. T. and Davies, M. J. (1999) Histone H1- and other protein- and amino acid-hydroperoxides can give rise to free radicals which oxidize DNA. Biochem. J. **344**, 125–134
6 Stadtman, E. R. (1995) Role of oxidized amino acids in protein breakdown and stability. Methods Enzymol. **258**, 379–393
7 Dean, R. T., Fu, S., Stocker, R. and Davies, M. J. (1997) Biochemistry and pathology of radical-mediated protein oxidation. Biochem. J. **324**, 1–18
8 Liggins, J. and Furth, A. J. (1997) Role of protein-bound carbonyl groups in the formation of advanced glycation endproducts. Biochim. Biophys. Acta **1361**, 123–130
9 Fu, S., Fu, M. X., Baynes, J. W., Thorpe, S. R. and Dean, R. T. (1998) Presence of dopa and amino acid hydroperoxides in proteins modified with advanced glycation end products (AGEs): amino acid oxidation products as a possible source of oxidative stress induced by AGE proteins. Biochem. J. **330**, 233–239
10 Pleshakova, O. V., Kutsyi, M. P., Sukharev, S. A., Sadovnikov, V. B. and Gaziev, A. I. (1998) Study of protein carbonyls in subcellular fractions isolated from liver and spleen of old and gamma-irradiated rats. Mech. Ageing Dev. **103**, 45–55
11 Ullrich, O., Reinheckel, T., Sitte, N., Hass, R., Grune, T. and Davies, K. J. (1999) Poly-ADPribose polymerase activates nuclear proteasome to degrade oxidatively damaged histones. Proc. Natl. Acad. Sci. U.S.A. **96**, 6223–6228
12 Gugliucci, A. and Bendayan, M. (1995) Histones from diabetic rats contain increased levels of advanced glycation end products. Biochem. Biophys. Res. Commun. **212**, 56–62
13 Medina, L. and Haltiwanger, R. S. (1998) Calf thymus high mobility group proteins are nonenzymatically glycated but not significantly glycosylated. Glycobiology **8**, 191–198
14 Takata, K., Horiuchi, S., Araki, N., Shiga, M., Saitoh, M. and Morino, Y. (1988) Endocytic uptake of nonenzymatically glycosylated proteins is mediated by a scavenger receptor for aldehyde-modified proteins. Biochemistry **263**, 14819–14825
15 Johns, E. W. (1964) Studies on histones. 7. Preparative methods for histone fractions from calf thymus. Biochem. J. **92**, 55–59
16 Bonnieu, A., Rech, J., Jeanteur, P. and Fort, P. (1989) Requirements for c-fos mRNA down regulation in growth stimulated murine cells. Oncogene **4**, 881–888
17 Ruiz-Carillo, A. and Jorcano, J. L. (1979) An octamer of core histones in solution: central role of the H3-H4 tetramer in the self-assembly. Biochemistry **18**, 760–768
18 Chao, C. C., Ma, Y. S. and Stadtman, E. R. (1997) Modification of protein surface hydrophobicity and methionine oxidation by oxidative systems. Proc. Natl. Acad. Sci. U.S.A. **94**, 2969–2974
19 Cervantes-Laurean, D., Jacobson, E. L. and Jacobson, M. K. (1996) Glycation and glycoxidation of histones by ADP-ribose. J. Biol. Chem. **271**, 10461–10469
20 Shacter, E., Williams, J. A., Lim, M. and Levine, R. L. (1994) Differential susceptibility of plasma proteins to oxidative modification: examination by western blot immunoassay. Free Radical Biol. Med. **17**, 429–437
21 Lenz, A. G., Costabel, U., Shaltiel, S. and Levine, R. L. (1989) Determination of carbonyl groups in oxidatively modified proteins by reduction with tritiated sodium borohydride. Anal. Biochem. **177**, 419–425
22 Jacobson, M. K., Levi, V., Juarez-Salinas, H., Barton, R. A. and Jacobson, E. L. (1980) Effect of carcinogenic *N*-alkyl-*N*-nitroso-compounds on nicotinamide adenine dinucleotide metabolism. Cancer Res. **40**, 1797–1802
23 Jacobson, E. L., Antol, K. M., Juarez-Salinas, H. and Jacobson, M. K. (1983) Poly(ADP-ribose) metabolism in UV irradiated human fibroblasts. J. Biol. Chem. **258**, 102–107
24 Jacobson, E. L., Cervantes-Laurean, D. and Jacobson, M. K. (1997) ADP-ribose in glycation and glycoxidation reactions. Adv. Exp. Med. Biol. **419**, 371–379
25 Shearman, M. S., Ragan, C. I. and Iversen, L. L. (1994) Inhibition of PC12 cell redox activity is a specific, early indicator of the mechanism of beta-amyloid-mediated cell death. Proc. Natl. Acad. Sci. U.S.A. **91**, 1470–1475
26 Elgawish, A., Glomb, M., Friedlander, M. and Monnier, V. M. (1996) Involvement of hydrogen peroxide in collagen cross-linking by high glucose *in vitro* and *in vivo*. J. Biol. Chem. **271**, 12964–12971
27 Edelstein, D. and Brownlee, M. (1992) Mechanistic studies of advanced glycosylation end product inhibition by aminoguanidine. Diabetes **41**, 26–29
28 Silverstein, R. M., Bassler, G. C. and Morril, T. C. (1991) ^{13}C-NMR spectroscopy. In Spectrometric Identification of Organic Compounds, pp. 227–265, John Wiley & Sons, New York
29 Cervantes-Laurean, D., Minter, D. E., Jacobson, E. L. and Jacobson, M. K. (1993) Protein glycation by ADP-ribose: studies of model conjugates. Biochemistry **32**, 1528–1534
30 Acharya, A. S. and Manning, J. M. (1980) Amadori rearrangement of glyceraldehyde-hemoglobin Schiff base adducts. A new procedure for the determination of ketoamine adducts in proteins. J. Biol. Chem. **255**, 7218–7224
31 Stadtman, E. R. (1992) Protein oxidation and aging. Science **257**, 1220–1224
32 Levine, R. L., Williams, J. A., Stadtman, E. R. and Shacter, E. (1994) Carbonyl assays for determination of oxidatively modified proteins. Methods Enzymol. **233**, 346–357
33 Yan, L. J., Levine, R. L. and Sohal, R. S. (1997) Oxidative damage during aging targets mitochondrial aconitase. Proc. Natl. Acad. Sci. U.S.A. **94**, 11168–11172
34 Wolffe, A. P. (1992) Chromatin structure. In Chromatin Structure and Function, pp. 4–67, Academic Press, London
35 Oliver, C. N., Ahn, B.-W., Moerman, E. J., Goldstein, S. and Stadtman, E. R. (1987) Age-related changes in oxidized proteins. J. Biol. Chem. **262**, 5488–5491
36 Commerford, S. L., Carsten, A. L. and Cronkite, E. P. (1982) Histone turnover within nonproliferating cells. Proc. Natl. Acad. Sci. U.S.A. **79**, 1163–1165
37 Ullrich, O., Sitte, N., Sommerburg, O., Sandig, V., Davies, K. J. A. and Grune, T. (1999) Influence of DNA binding on the degradation of oxidized histones by the 20S proteasome. Arch. Biochem. Biophys. **362**, 211–216
38 Kreimeyer, A., Wielkens, P., Adamietz, P. and Hilz, H. (1984) DNA repair-associated ADP-ribosylation *in vivo*. Modification of histone H1 differs from that of the principal acceptor proteins. J. Biol. Chem. **259**, 890–896
39 Strahl, B. D. and Allis, C. D. (2000) The language of covalent histone modifications. Nature (London) **403**, 41–45
40 Enright, H. U., Miller, W. J. and Hebbel, R. P. (1992) Nucleosomal histone protein protects DNA from iron-mediated damage. Nucleic Acids Res. **20**, 3341–3346
41 Chol Ha, H., Sirisoma, N. S., Kuppusamy, P., Zweier, J. L., Woster, P. M. and Casero, R. A. (1998) The natural polyamine spermine functions directly as a free radical scavenger. Proc. Natl. Acad. Sci. U.S.A. **95**, 11140–11145

Received 8 May 2000/26 June 2000; accepted 24 July 2000